Effects of Pressure Gradients and Streamline Curvature on Turbulent Pipe Flow
Version 1: 1 February 2020

Test Case Coordinators

Alexander J. Smits and Marcus Hultmark

Princeton University, US

E-mail : asmits@princeton.edu, hultmark@Princeton.edu, liuyangd@princeton.edu

Phone: 609 258 5117

Student Contacts: Alexander Pique, Simeret Genet

Princeton University, US
E-mail: apique@princeton.edu, sgenet@princeton.edu

Introduction

The purpose of this work is to extend our knowledge on canonical wall-bounded turbulence (constrained by parallel walls or a flat plate) to flows experiencing changing boundary conditions. In particular, when there are curved boundaries and/or non-constant cross-sectional areas, pressure gradients and streamline curvature play important roles in turbulence production, dissipation and transport.

Methods expected to be benchmarked for this test case include
- Flow modeling methods such as RANS or Hybrid RANS/LES & WMLES
- Flow simulation methods such as WRLES or DNS

In the present work, a fully developed turbulent pipe flow is perturbed by a streamlined axisymmetric body placed on the centerline, introducing a spatially-varying pressure gradient and streamline curvature. We will examine the response of the flow to combined pressure and curvature effects, as well as the recovery behavior downstream. The purpose of this test case is to benchmark turbulent boundary layer development and fluctuating turbulent wall pressure on a smooth wall in the presence of a systematic family of adverse and favorable pressure gradient cases. Preliminary results were presented at TSFP 11 in Southampton (attached to this document, and listed in the references).

Test Description

Figure 1 illustrates the test configuration. A streamlined axisymmetric body was placed on the centerline of a pipe that has an inner diameter of $D = 2R = 38.1$ mm. The body consisted of three sections -- the bow ($0<x/R<2.67$), stern ($10<x/R<12.67$) and cylindrical recovery

(2.67$<x/R<10) sections. Currently available measurements are confined to the bow and recovery sections. The stern section and the downstream recovery region will be examined in the next phase. The bow section is an 8:1 prolate spheroid; the contour of the stern follows a 4th-order power law to minimize the drag. With the presence of the body, the incoming flow experienced FPG and convex curvature over the bow, followed by relaxation in the recovery section, and then entered the stern region with APG and convex curvature. Three body diameters, d=D/3, √2D/3 and √3D/3 were chosen to vary the magnitude and rate of change of pressure and curvature, where d is the diameter of the body of revolution. The inflow was fully developed pipe flow by allowing a development length of 200D upstream of the body.

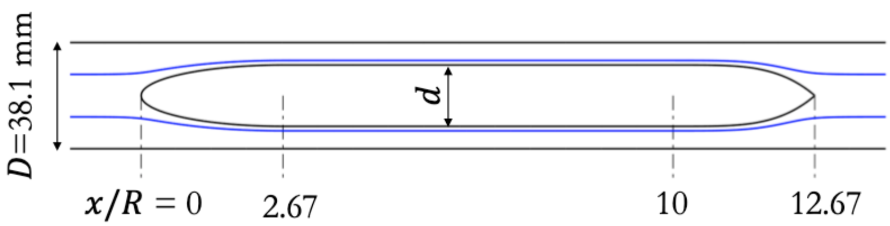

Figure 1. Test section geometry. Three body sizes were tested: d=D/3, √2D/3 and √3D/3. Flow is from left to right.

We conducted planar particle image velocimetry (PIV) in the axial-radial plane to study the evolution of turbulence. The body was supported by an airfoil-shaped (NACA0015) sting. The pipe facility operated at a bulk velocity of 4.1 m/s, corresponding to Re_D = 156,000 at ambient temperature (20^{o}C). The upstream friction velocity was 0.186 m/s, and Ret = 3550.

<u>**Overall Test Section Conditions**</u>

Based on the geometry of the bodies and the conservation of mass, we can calculate the bulk velocity at any axial location. The acceleration factor, $K_b = (\nu/U_b^2)\, dU_b/dx$, is plotted in figure 2a. It may be seen that K_b at x=0 for the three bodies varies approximately in the ratio 1:2:3, that is, it scales approximately with d^2. However, the largest body creates a non-monotonic K_b peaking at x/R=0.6, while for the medium and small bodies K_b monotonically decreases to zero.

Figure 2b shows the curvature (the reciprocal of local radius of curvature, 1/|a|) of streamlines for -0.3<x/R<0.3 at different radial locations. Only the results for the large body are shown, but for the small and medium bodies the variation of curvature is qualitatively the same but less dramatic. It is clear that the curvature effect is strong near the body surface (r small) and fades towards the outer wall, and that a rapid switch from concave to convex curvature occurs near x = 0. In fact, the flow behavior in this region is even more complicated because, in addition to the curvature, there also exists a strong APG as the flow approaches the tip of the body. The combined deceleration and curvature effect poses an interesting question to the response of turbulence, for which we will gain some insights from our later discussion on the Reynolds shear stress. Further downstream (0.3<x/R<2.67, not shown here), the flow sees convex curvature with the magnitude decreasing in both the axial and radial directions.

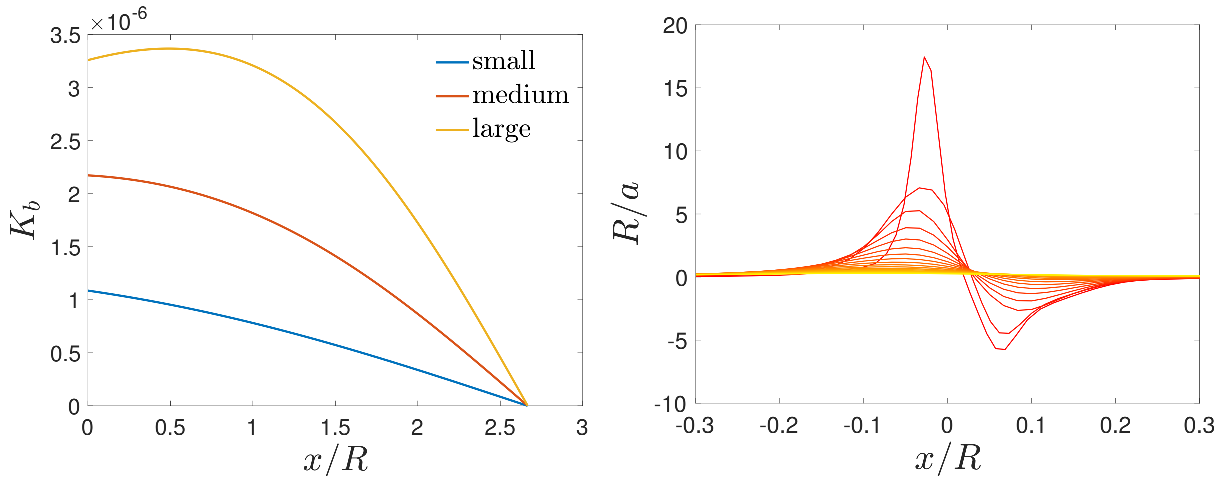

Figure 2: Left: Acceleration factor K_b based on the bulk velocity. Right: Curvature of streamlines near x = 0 of the large body at different radial locations, where r increases from red to yellow. Here, |a| is the local radius of curvature (a>0 and a<0 represent concave and convex curvature, respectively).

Overall Form of the Flow Response

Setails on the response of the mean flow, the streamwise and radial component of the turbulence, and the Reynolds shear stress are available from the TSFP 11 presentations, listed in the references and attached to this document.

Preliminary Conclusions on the Measurements

We investigated a turbulent pipe flow at Re_D = 156,000$ passing over different bodies of revolution placed on the centerline. Each body had a streamlined shape introducing a favorable pressure gradient and convex streamline curvature to the flow over the bow section. The flow subsequently underwent recovery through a circular annulus formed by the pipe wall and the constant area mid-section of the body.

The mean streamwise velocity in the bow section exhibited a linear distribution in the range where a logarithm law is expected for fully developed flows. The linear distribution was observed over the major part of the bow section.

The production by Reynolds shear stress appeared to be responsible for the formation of the linear distribution of the mean velocity. We found strong negative Reynolds stress near the body wall at the beginning of the bow section, which strengthened the velocity gradient to form the linear distribution, as opposed to the velocity gradient of the equilibrium flow which continuously decreases towards the pipe center.

The strong negative Reynolds stress, which indicated energized turbulence, resulted from the strong deceleration and streamline divergence prior to the bow tip. We analyzed the transport equation of Reynolds stress to explain the strong production of Reynolds shear stress in this region.

In mid-body recovery section, the flow underwent a slow recovery process. The variation near the walls was more pronounced, but overall the flow only changed slightly. The recovery process was therefore expected to continue for a long distance.

The authors gratefully acknowledge the support under ONR Grant ``Understanding Turbulence on Navy Vehicles" N00014-17-1-2309 (Program Manager Peter Chang.

Additional Measurements to be made

(a) Currently available measurements are confined to the bow and recovery sections. The stern section and the downstream recovery region will be examined in the next phase.
(b) Measurements at much higher Reynolds numbers (Re_D up to 6 x 10^6) are planned for the Princeton Superpipe facility. A new traversing system has been designed and installed, and a PIV system for this high pressure environment has been designed (Ding et al. 2020).

References

[1] Ding, L., Saxton-Fox, T., Hultmark, M. and Smits, A. J. “Effects of pressure gradient and streamline curvature on the statistics of a turbulent pipe flow,” 11th International Symposium on Turbulence and Shear Flow Phenomena, Southampton UK, July 30-Aug 2, 2019.
[2] Saxton-Fox, T., Ding, L., Smits, A. J. and Hultmark, M. “Coherent structure deformation in a turbulent pipe flow with a spatially-developing pressure gradient,” 11th International Symposium on Turbulence and Shear Flow Phenomena, Southampton UK, July 30-Aug. 2, 2019.
[3] Ding, L., Hultmark, M. and Smits, A. J. “A New Stereoscopic PIV System For The Princeton Superpipe,” 20th International Symposium on Applications of Laser Techniques to Fluid Mechanics, Lisbon, Portugal, July 13-16, 2020.